

# Free-Fermionic Topological Quantum Sensors

Saubhik Sarkar,<sup>1,\*</sup> Chiranjib Mukhopadhyay,<sup>2,3,†</sup> Abhijeet Alase,<sup>1,‡</sup> and Abolfazl Bayat<sup>3,§</sup>

<sup>1</sup>*Institute for Quantum Science and Technology and Department of Physics and Astronomy,  
University of Calgary, Calgary, Alberta T2N 1N4, Canada*

<sup>2</sup>*RCQI, Institute of Physics, Slovak Academy of Sciences, Dúbravská cesta 9, 84511 Bratislava, Slovakia*

<sup>3</sup>*Institute of Fundamental and Frontier Sciences, University of Electronic Science and Technology of China, Chengdu 610051, China*

Second order quantum phase transitions, with well-known features such as long-range entanglement, symmetry breaking, and gap closing, exhibit quantum enhancement for sensing at criticality. However, it is unclear which of these features are responsible for this enhancement. To address this issue, we investigate phase transitions in free-fermionic topological systems that exhibit neither symmetry-breaking nor long-range entanglement. We analytically demonstrate that quantum enhanced sensing is possible using topological edge states near the phase boundary. Remarkably, such enhancement also endures for ground states of such models that are accessible in solid state experiments. We illustrate the results with 1D Su-Schrieffer-Heeger chain and a 2D Chern insulator which are both experimentally accessible. While neither symmetry-breaking nor long-range entanglement are essential, gap closing remains as the major candidate for the ultimate source of quantum enhanced sensing. In addition, we also provide a fixed and simple measurement strategy that achieves near-optimal precision for sensing using generic edge states irrespective of the parameter value. This paves the way for development of topological quantum sensors which are expected to also be robust against local perturbations.

*Introduction.*— The sensitivity of quantum systems to the variation of their environment makes them excellent sensors [1]. The uncertainty of measuring an unknown parameter  $\lambda$ , quantified by standard deviation  $\delta\lambda$  is bounded by Cramér-Rao inequality  $\delta\lambda \leq 1/\sqrt{MF}$ , where  $M$  is the number of trials and  $F$  is the Fisher information [2]. In a classical setup, the Fisher information scales linearly with the sensor size (known as standard limit). However, quantum features, such as superposition, may enhance the resource efficiency of a quantum sensor such that the Fisher information scales quadratically with system size (known as Heisenberg limit) [2], or even faster (super-Heisenberg limit) [3–8]. There are at least two major approaches for achieving quantum enhanced sensing: (i) exploiting GHZ-type entangled states [9–14] for estimating the angle of a unitary rotation [3]; and (ii) utilizing quantum criticality for directly estimating the Hamiltonian parameters [15–24]. In the former, the interaction between the particles in the quantum sensor degrades the sensing quality [24–27]. Also, because of extreme vulnerability of GHZ states to decoherence and particle loss, it is difficult to be scaled up [28]. In the latter, however, the interaction between the constituents of the quantum sensor is crucial and the system is more robust against decoherence. Originally the criticality-enhanced quantum sensing has been introduced for the ground state of many-body systems undergoing a second order quantum phase transition [15–24]. In such symmetry breaking transitions, the ground state reveals long-range correlations which lead to the scaling of  $F \sim V^{2/D\nu}$ , where  $V$  is the system size (volume),  $D$  is the dimension, and  $\nu$  is the critical exponent with which the correlation length diverges near the criticality [3]. Recently, quantum enhanced sensing has also been observed in integrable Floquet systems [7, 29] along the line that the Floquet gap vanishes. An important open question is what feature of a phase transition, e.g. symmetry breaking, long-range correlations, or vanishing gap, is truly responsible for obtaining quantum enhanced sensing.

To answer this, one needs to investigate the scaling of Fisher information in different types of quantum phase transitions, e.g. those not of symmetry-breaking kind. Phase transitions in symmetry-protected topological (SPT) phases of non-interacting fermions [30, 31] are ideal candidates for this investigation. These topological phase transitions (TPT) are fundamentally different from the symmetry-breaking ones in at least three aspects [32]. First, a fermionic SPT phase transition manifests in the form of robust edge/surface states protected against symmetry-preserving local perturbations [33–35]. Second, they are not characterized by a jump in the value or the derivative of a local order parameter, but rather by an integer-valued jump in a global quantity that is called a topological invariant [32]. Third, unlike the symmetry-breaking phase transitions, the fermionic SPT phases at TPT are short-range entangled [36]. These differences between second-order phase transitions and fermionic SPT phase transitions motivate our investigation of quantum enhanced sensitivity in the latter. In fact, sensing based on non-Hermitian topological systems [37] and TPTs for rotation angle estimation [38–43] (like GHZ state-based metrology) have been already proposed. Nonetheless, the sensing capability of free-fermionic TPTs for estimating Hamiltonian parameters is yet to be explored. From an experimental perspective, fermionic SPT phases have been observed in various systems such as integer quantum Hall effect [44] and topological insulators [45], as well as simulated using various experimental platforms including ultracold atoms [46] and photonics [47]. Therefore, finding quantum enhanced precision in such systems is a key step forward for developing topological quantum sensors.

In this Letter, we analytically address the quantum sensing capability of free-fermionic topological systems across phase transitions. We have two main findings. Firstly, from a practical perspective, we show that these systems indeed reveal quantum enhanced sensitivity and thus are legitimate candidates for developing topological quantum sensors, which are

naturally robust against local perturbations. Secondly, from a fundamental perspective, we highlight the importance of gap closing, as opposed to symmetry-breaking or long-range entanglement, for quantum enhanced sensing.

*Ultimate precision limit.*— To infer an unknown parameter  $\lambda$ , encoded in a quantum state  $\rho_\lambda$ , one has to perform measurement on the system and then feed the outcomes into an estimator algorithm. For a given measurement setup, described by a set of projective operators  $\{\Pi_n\}$ , every outcome appears with the probability  $p_n(\lambda) = \text{Tr}[\rho_\lambda \Pi_n]$ . In this case, all the information is encoded in a classical probability distribution and thus the Cramér-Rao bound is determined by Classical Fisher Information (CFI), defined as  $F^C = \sum_k p_n(\partial_\lambda \log p_n)^2$ . One can maximize the CFI for all possible measurement setups to obtain Quantum Fisher Information (QFI) as the ultimate precision bound. The QFI can be computed as  $F^Q = \text{Tr}[\mathcal{L}_\lambda^2 \rho_\lambda]$ , where  $\mathcal{L}_\lambda$  is the Symmetric Logarithmic Derivative (SLD) operator defined as  $\partial_\lambda \rho_\lambda = (\rho_\lambda \mathcal{L}_\lambda + \mathcal{L}_\lambda \rho_\lambda)/2$ . For pure states  $\rho_\lambda = |\psi_\lambda\rangle\langle\psi_\lambda|$ , SLD operator simplifies to  $\mathcal{L}_\lambda = 2\partial_\lambda \rho_\lambda$ , and  $F^Q = 4(\langle\partial_\lambda \psi_\lambda|\partial_\lambda \psi_\lambda\rangle - |\langle\partial_\lambda \psi_\lambda|\psi_\lambda\rangle|^2)$  [2]. It is worth emphasizing that the optimal measurement setup that achieves the ultimate precision bound is not unique, although one solution is always given by the eigenvectors of the SLD operator.

*Free-fermionic SPT model.*— Free-fermionic SPT phases host energy excitations localized on the boundary known as edge/surface states. The existence of these edge/surface states is guaranteed by the non-trivial topology of the filled band wavefunctions [33, 34]. These edge/surface states are studied using tight-binding models [48–51]. We first analyze the QFI of the edge states in 1D systems and later generalize our results to higher dimensions. Consider a 1D lattice with sites labeled by  $\{j : j \in [L]\}$ , where  $[L] = \{0, 1, \dots, L-1\}$ . Suppose there are  $d$  internal degrees of freedom associated to each lattice site. The single-particle Hilbert space  $\mathcal{H}$  is then spanned by orthonormal basis states  $\{|j, m\rangle : j \in [L], m \in [d]\}$ , and can be tensor-factorized as  $\mathcal{H} \cong \mathcal{H}_L \otimes \mathcal{H}_1$  [48, 49]. The single-particle Hamiltonian of a number-conserving, non-interacting fermionic system with uniform coupling and open boundary conditions (OBC) can be expressed as

$$H = \sum_{j \in [L]} |j\rangle\langle j| \otimes h_0(\lambda) + \sum_{j < j' \in [L]} (|j\rangle\langle j'| \otimes h_{j'-j}(\lambda) + \text{H.c.}), \quad (1)$$

where each  $h_{j'-j}$  is a  $d \times d$  matrix whose entries are complex amplitudes of hopping between lattice sites separated by distance  $j' - j$  possibly accompanied by a change in internal state [48, 49], and these entries depend on the parameter  $\lambda$  that is being estimated. Hamiltonians of the form in Eq. (1) are routinely used for investigation of edge states in 1D free-fermionic topological systems. Our analysis can be generalized to number non-conserving systems including Kitaev chain [52], as Bogoliubov de-Gennes Hamiltonian of such systems has the same structure as in Eq. (1).

*Edge states in 1D.*— The zero-energy edge states (topologically protected or accidental) localized on the  $j = 0$  edge are

described (or well-approximated) by  $|\psi_{\text{edge}}\rangle = |\phi_z\rangle|u\rangle$ , where

$$|\phi_z\rangle = \sqrt{\frac{1-|z|^2}{1-|z|^{2L}}} \sum_{j \in [L]} z^j |j\rangle, \quad z \in \mathbb{C}, |z| < 1 \quad (2)$$

parametrized by the complex number  $z$  accounts for the spatial part of exponentially decaying nature of the wavefunction, and  $|u\rangle \in \mathcal{H}_1$  is an internal state vector [48–50]. Note that both  $z$  and  $|u\rangle$  depend on  $\lambda$  in general.

We now derive the scaling of QFI for  $|\psi_{\text{edge}}\rangle$ , assuming  $\arg(z)$  is independent of  $\lambda$ , and leave the general case for the supplemental material (SM) [53]. We state this and other results using  $O$ ,  $\Omega$ , and  $\Theta$  asymptotic notations, which are used to state upper, lower, and tight bounds on the scaling respectively [54]. The QFI for  $|\psi_{\text{edge}}\rangle$  with respect to  $\lambda$  can be expressed as  $F_{|\psi_{\text{edge}}\rangle}(\lambda) = F_{|\phi_z\rangle}(\lambda) + F_{|u\rangle}(\lambda)$ . For  $L \gg 1$ , both  $z$  and  $|u\rangle$  approach a fixed value that does not depend on  $L$  [48, 49]. However, the state  $|\phi_z\rangle$  depends on  $L$  due to the normalization. Therefore, the scaling of QFI comes from the scaling of  $F_{|\phi_z\rangle}(\lambda) = 4(\langle\partial_\lambda \phi_z|\partial_\lambda \phi_z\rangle - |\langle\partial_\lambda \phi_z|\phi_z\rangle|^2)$ . Note that  $\langle\partial_\lambda \phi_z|\phi_z\rangle = 0$  for  $\arg(z)$  independent of  $\lambda$ , and simple algebra reveals

$$F_{|\phi_z\rangle}(\lambda) = \frac{4(\partial_\lambda |z|)^2 [1 + |z|^{4L} - |z|^{2L-2}(2|z|^2 + L^2(1 - |z|^2)^2)]}{(1 - |z|^2)^2(1 - |z|^{2L})^2}. \quad (3)$$

Away from TPT,  $|z| < 1$  yields  $\lim_{L \rightarrow \infty} F_{|\phi_z\rangle}(\lambda) = 4(\partial_\lambda z)^2(1 - z^2)^{-2}$ , so that  $F_{|\psi_{\text{edge}}\rangle}(\lambda) \in \Theta(1)$ . As edge states are localized single particle excitations, we do not expect  $L$ -dependent scaling away from TPT. In contrast, at TPT, the zero-energy edge states undergo delocalization, so that  $|z| \rightarrow 1$  as  $\lambda$  approaches the transition point  $\lambda_c$  [48, 49]. Consequently, by calculating the limit of Eq. (3) as  $\lambda \rightarrow \lambda_c$ , we get

$$\lim_{\lambda \rightarrow \lambda_c} F_{|\phi_z\rangle}(\lambda) = \frac{(\partial_\lambda z)^2(L^2 - 1)}{3} \implies F_{|\psi_{\text{edge}}\rangle}(\lambda_c) \in \Theta(L^2), \quad (4)$$

independent of the model Hamiltonian. The same result holds for complex  $z$ , as we show in the SM [53]. This quadratic scaling of the QFI of edge states at the phase transition is a remarkable observation showing the power of free-fermionic topological systems for achieving quantum enhanced sensitivity. This is in fact the first main result of our work.

*Edge states in higher dimensions.*— We now investigate the scaling of the QFI of the edge states of  $D$ -dimensional systems in which periodic boundary conditions (PBC) are enforced along  $D-1$  directions, and OBC along the remaining direction. For ease of explanation, consider a 2D square lattice with the orthonormal basis states  $\{|j_1, j_2, m\rangle : j_1 \in [L_1], j_2 \in [L_2], m \in [d]\}$  [51]. A Hamiltonian with PBC along both the spatial directions can be expressed as  $H_{\text{PBC}} = \oplus_{\mathbf{k}} H_{\mathbf{k}}$  of a topological system with  $\mathbf{k}$  in the two-dimensional Brillouin zone and  $H_{\mathbf{k}}$  the Bloch Hamiltonian [55]. If instead of PBC, OBC is enforced along the first spatial direction, then  $\mathbf{k}$  is no longer a good quantum number. However,  $k_{\parallel}$  (component of  $\mathbf{k}$  along the periodic direction) remains a good quantum number, and therefore the total Hamiltonian can be expressed as  $H_{\text{OBC}} = \oplus_{k_{\parallel}} H_{k_{\parallel}}$ , with  $H_{k_{\parallel}}$  denoting the Hamiltonian of a virtual

1D wire labeled by  $k_{\parallel}$  [51]. Each  $H_{k_{\parallel}}$  has a structure similar to that of the Hamiltonian in Eq. (1). An edge state  $|\psi_{\text{edge}}\rangle$  at a fixed  $k_{\parallel}$  is well-approximated by  $|\psi_{\text{edge}}\rangle = |k_{\parallel}\rangle |\phi_z\rangle |u(z, k_{\parallel})\rangle$ , where  $|\phi_z\rangle$  is given in Eq. (2) with the replacement  $L \rightarrow L_2$ , and  $|k_{\parallel}\rangle = \frac{1}{\sqrt{L_1}} \sum_{j_1 \in [L_1]} e^{ik_{\parallel}j_1} |j_1\rangle$  with  $k_{\parallel} \in [-\pi, \pi)$  is a crystal momentum eigenstate. For an edge state at a fixed value of  $k_{\parallel}$ , we have  $\partial_{\lambda} |k_{\parallel}\rangle = 0$ , and therefore  $F_{|\psi_{\text{edge}}\rangle}(\lambda) = F_{|\phi_z\rangle}(\lambda) + \text{constant} \in \Theta(L_2^2)$  at TPT as in the 1D case. Interestingly, for  $L_1=L_2=L$ , we have  $F_{|\psi_{\text{edge}}\rangle}(\lambda) \in \Theta(V)$  where  $V=L^2$  is the total system size (area). For  $D$ -dimensional system, lattice sites are indexed by  $\{j_1, \dots, j_D\}$ , and PBC are enforced along the first  $D-1$  directions. Similar analysis as above yields  $F_{|\psi_{\text{edge}}\rangle}(\lambda) \in \Theta(V^{2/D})$  at TPT, similar to the behaviour of QFI at second order phase transitions [3]. This establishes the scaling of QFI of edge states in any spatial dimension.

*Optimal measurement basis for edge states.*— While QFI determines the ultimate precision bound, its saturation in the Cramér-Rao inequality relies on the choice of an optimal measurement basis. For the case where  $\arg(z)$  is independent of  $\lambda$ , the position measurement is sufficient to saturate the Cramér-Rao bound for QFI  $F_{|\phi_z\rangle}(\lambda)$  for every  $\lambda$ .  $F_{|u\rangle}$  approaches a fixed value for  $L \gg 1$ . Consequently, as proved in the SM [53], the measurement of  $|\psi_{\text{edge}}\rangle$  performed in the basis

$$\mathcal{B} = \{|j\rangle \langle j| \otimes \mathbb{1}_d, j \in [L]\} \quad (5)$$

yields optimal precision up to a length-independent constant. In the SM [53], we show that this measurement also yields optimal precision up to a length-independent prefactor if  $\arg(z)$  depends on  $\lambda$ . Interestingly, the measurement basis  $\mathcal{B}$  is independent of  $\lambda$ , which makes sensing easier in practice.

*Example for 1D.*— As a concrete example we consider the Su-Schrieffer-Heeger (SSH) Hamiltonian [56]

$$\hat{H}^{\text{SSH}} = - \sum_{j \in [L]} \left( J_1 \hat{b}_j^\dagger \hat{a}_j + J_2 \hat{a}_{j+1}^\dagger \hat{b}_j + \text{H.c.} \right), \quad (6)$$

where,  $J_1$  is the coupling for exchanging the two internal states (denoted by fermionic operators  $\hat{a}_j$  and  $\hat{b}_j$  at site  $j$ ) at a single site and  $J_2$  is the coupling for exchanging the internal states between two adjacent sites. The single particle Hamiltonian is of the same form as in Eq. (1), for which  $h_0 = -J_1 \sigma_x$ , and  $h_1 = -J_2(\sigma_x - i\sigma_y)/2$ , with  $\sigma_x, \sigma_y$  being Pauli matrices, and all the other  $h$  matrices vanish. This model exhibits TPT at  $J_1 = J_2$  protected by sublattice symmetry, and has been realized in both solid state [56] and optical lattice [57] experiments. For simplicity, we shall assume that  $\hat{b}_{L-1}$  is isolated from other sites in the SSH chain [58], and  $\lambda = J_1/J_2$  is a real parameter which has to be estimated. For  $\lambda < \lambda_c = 1$ , the normalized edge state solution is given by [59]  $|\psi_{\text{edge}}^{\text{SSH}}\rangle = |\phi_{z=-\lambda}\rangle |u\rangle$ , where  $|\phi_z\rangle$  is given by Eq. (2) and  $|u\rangle = [1 \ 0]^T$ . We obtain the same scaling relation for QFI as in the general case. To verify this numerically, one can use a fit function  $aL^b + c$  to the QFI of  $|\psi_{\text{edge}}^{\text{SSH}}\rangle$  for each value of  $\lambda$  and extract the exponent  $b$ . As one moves away from TPT, scaling of QFI changes from quadratic ( $b=2$ ) to constant ( $b=0$ ), as

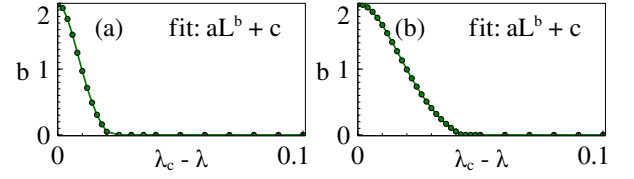


FIG. 1. Scaling exponent of QFI of edge state as a function of  $\lambda$  for (a) SSH model, and (b) Chern insulator model.

displayed in Fig. 1(a). Note that  $z$  is real and  $|u\rangle$  is constant, therefore the measurement described by Eq. (5) is optimal.

*Example for 2D.*— We now illustrate the scaling of QFI for a Chern insulator on a square lattice, which is a prototypical model of topological insulators with broken time-reversal symmetry [31]. This model has also been experimentally realized in optical lattices [60]. In second quantization, the Chern insulator Hamiltonian is [61, 62]

$$\hat{H}^{\text{Ch}} = \sum_{\mathbf{k}} \left[ \hat{c}_{\mathbf{k},\uparrow}^\dagger \hat{c}_{\mathbf{k},\downarrow}^\dagger \right] H_{\mathbf{k}}^{\text{Ch}} \left[ \hat{c}_{\mathbf{k},\uparrow} \hat{c}_{\mathbf{k},\downarrow} \right]^T, \quad (7)$$

where  $H_{\mathbf{k}}^{\text{Ch}} = \mathbf{B} \cdot \boldsymbol{\sigma}$  is the Bloch Hamiltonian with  $\mathbf{B} = (2t_1 \cos k_x, 2t_1 \cos k_y, m_z + 2t_2(\sin k_x + \sin k_y))$  and  $\boldsymbol{\sigma}$  the vector of Pauli matrices. Here  $\uparrow, \downarrow$  denote spin-1/2 up and down states, and  $m_z, t_1, t_2$  are lattice parameters. We will consider  $\lambda = m_z/t_2$  as the parameter to be estimated. The eigenvectors of this spin-orbit coupled Hamiltonian form two bands that touch at phase transition at the Dirac points  $(k_x, k_y) = \pm(\pi/2, \pi/2)$  for non-zero  $\lambda$ , and the corresponding phase boundaries are given by  $\lambda_c = \mp 4$  [62]. We impose PBC along  $x$  direction so that  $k_{\parallel} = k_x$ , and decompose the single-particle Hamiltonian as  $H^{\text{Ch}} = \oplus_{k_x} H_{k_x}$ , where  $H_{k_x}$  describes a virtual 1D wire Hamiltonian of the form in Eq. (1) with  $h_0(k_x) = 2t_1 \cos k_x \sigma_x + (m_z + 2t_2 \sin k_x) \sigma_z$ ,  $h_1(k_x) = t_1 \sigma_y - it_2 \sigma_z$ . The QFI of the edge state at  $k_x = \pi/2$  localized near  $j = 0$ , displayed in Fig. 1(b), shows quadratic scaling at TPT and constant scaling away from it.

As edge states are single-particle states unaffected by exchange statistics, quantum-enhanced sensitivity is expected for both non-interacting fermionic and bosonic systems. Edge-state based sensing requires populating the edge states without populating the bulk, which has already been achieved experimentally in bosonic systems [63–66].

*QFI of many-body ground state.*— We now look at the scaling nature for the fermionic many-body ground states, which are relevant for solid state experiments. We first derive a formula for the QFI of a general many-body state  $|\Psi\rangle$  of  $N$  fermions occupying single-particle states denoted by  $|\psi_1\rangle, \dots, |\psi_N\rangle$ . The anti-symmetrized wavefunction for this state is given by the Slater determinant formula [67]  $|\Psi\rangle = (1/\sqrt{N!}) \sum_{\sigma \in S_N} \text{sgn}(\sigma) |\psi_{\sigma_1}\rangle \dots |\psi_{\sigma_N}\rangle$  where  $S_N$  is the symmetric group. The QFI of this state simplifies to (see SM [53])

$$F_{|\Psi\rangle} = 4 \sum_l \langle \partial_{\lambda} \psi_l | \mathbb{1} - P | \partial_{\lambda} \psi_l \rangle, \quad (8)$$

with the projector on the occupied states  $P = \sum_{l=1}^N |\psi_l\rangle \langle \psi_l|$ .

For a large enough system, the scaling of QFI of the ground state should be independent of the boundary conditions. Hence, we focus on the case of PBC for analytical calculations. Afterwards, we numerically validate that our findings carry over to the OBC case. Consider the ground state of a  $D$ -dimensional free-fermionic Hamiltonian under PBC, with filling fraction adjusted such that the lowest energy band is filled and all other energy bands are empty. Translational invariance dictates that each single-particle state in the filled band is of the form  $|\psi_{\mathbf{k}}\rangle = |\mathbf{k}\rangle|u_{\mathbf{k}}\rangle$ , where  $|\mathbf{k}\rangle$  is the plane-wave state. Then we have  $|\partial_{\lambda}\psi_{\mathbf{k}}\rangle = |\mathbf{k}\rangle|\partial_{\lambda}u_{\mathbf{k}}\rangle$ . Eq. (8) then simplifies to

$$F_{\text{GS}}^{\text{PBC}} = 4 \sum_{\mathbf{k}} \left( \langle \partial_{\lambda}u_{\mathbf{k}} | \partial_{\lambda}u_{\mathbf{k}} \rangle - |\langle \partial_{\lambda}u_{\mathbf{k}} | u_{\mathbf{k}} \rangle|^2 \right) = \sum_{\mathbf{k}} F_{|u_{\mathbf{k}}\rangle}. \quad (9)$$

We now investigate the scaling behavior of  $F_{\text{GS}}^{\text{PBC}}$ .

*Many-body QFI at TPT.*— We now show how  $\Omega(L^2)$  scaling of  $F_{\text{GS}}^{\text{PBC}}$  emerges at TPT in a simplistic model of band-gap inversion in 1D systems [32]. Consider a two-band Hamiltonian that can be approximated as  $H_k = \alpha k \sigma_x + (\lambda - \lambda_c) \sigma_z$  near the Dirac point  $k = 0$ , with  $\alpha$  a Hamiltonian parameter independent of  $\lambda$  and  $L$ . The two energy bands touch at  $k=0$  at TPT (i.e.  $\lambda = \lambda_c$ ). Major contribution to QFI is expected from the states near the Dirac point. At Dirac point, we have  $H_{k=0} = (\lambda - \lambda_c) \sigma_z$ . For  $\lambda \geq \lambda_c$ , we have,  $|u_{k=0}\rangle = [0 \ 1]^T$ , and  $|\partial_{\lambda}u_{k=0}\rangle = 0$ , resulting in,  $F_{|u_{k=0}\rangle} = 0$ . We next look at the QFI of  $|u_1\rangle = |u_{k=2\pi/L}\rangle$  corresponding to  $k = 2\pi/L$  which is the closest point to the Dirac point in the Brillouin zone. Here  $H_k = \alpha(2\pi/L)\sigma_x + (\lambda - \lambda_c)\sigma_z$ , so that

$$|u_1\rangle = \begin{bmatrix} \cos(\gamma/2) \\ \sin(\gamma/2) \end{bmatrix}, \quad \text{and} \quad |\partial_{\lambda}u_1\rangle = \frac{\partial_{\lambda}\gamma}{2} \begin{bmatrix} -\sin(\gamma/2) \\ \cos(\gamma/2) \end{bmatrix}, \quad (10)$$

with  $\tan \gamma = \alpha/(\lambda - \lambda_c)$ . We now obtain  $F_{|u_1\rangle} = (\partial_{\lambda}\gamma)^2$ . By differentiating the expression for  $\tan \gamma$ , we get

$$\partial_{\lambda}\gamma = \frac{-\alpha/L}{(\lambda - \lambda_c)^2 + \alpha^2/L^2} \implies \lim_{\lambda \rightarrow \lambda_c} \partial_{\lambda}\gamma = -L/\alpha. \quad (11)$$

Therefore, at TPT,  $F_{|u_1\rangle} = L^2/\alpha^2 \in \Theta(L^2)$ . Now Eq. (9) rules out sub-quadratic scaling of  $F_{\text{GS}}^{\text{PBC}}$ , so that  $F_{\text{GS}}^{\text{PBC}} \in \Omega(L^2)$ .

To explicitly see this scaling behaviour at TPT we look at our prototypical examples of 1D SSH chain and 2D Chern insulator mentioned before. In the first case (see SM [53])

$$F_{\text{PBC}}^{\text{SSH}}(\lambda_c) = \sum_{\kappa=1}^{L-1} \frac{\cot^2(\pi\kappa/L)}{4} = \frac{L^2 - 3L + 2}{12}, \quad (12)$$

which clearly shows the  $\Theta(L^2)$  scaling for large  $L$ . Moreover, the Fock basis is an optimal measurement basis, as the ground state of SSH Hamiltonian has real coefficients in that basis [59]. Such a measurement can be performed by measuring the number operator  $\hat{c}_{j,m}^{\dagger} \hat{c}_{j,m}$  for each fermionic mode.

In the case of the Chern insulator, taking a  $L \times L$  lattice, QFI at TPT is given by (see SM [53])

$$F_{\text{PBC}}^{\text{Ch}}(\lambda_c) = \sum_{\mathbf{k} \neq (\pi/2, \pi/2)} \frac{B_x^2 + B_y^2}{4(B_x^2 + B_y^2 + B_z^2)}. \quad (13)$$

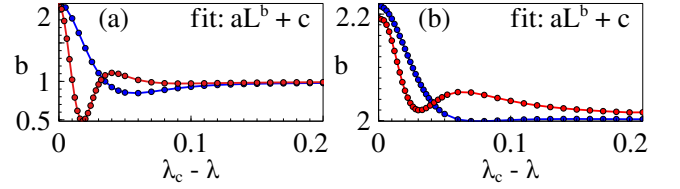


FIG. 2. Scaling exponent of QFI of many-body ground state as a function of  $\lambda$  subject to PBC (blue) and OBC (red) for (a) SSH model, and (b) Chern insulator model.

As we show later, this sum also shows  $\Omega(L^2)$  dependence.

*Many-body QFI away from TPT.*— We now investigate the scaling of  $F_{\text{GS}}^{\text{PBC}}$  away from the TPT. We prove that in this case,  $F_{|u_{\mathbf{k}}\rangle}$  is bounded by a constant independent of  $N$ , and therefore,  $F_{\text{GS}}^{\text{PBC}} \in O(N)$ , by Eq. (9). To derive this bound, first observe that  $F_{|u_{\mathbf{k}}\rangle} \leq 4 \langle \partial_{\lambda}u_{\mathbf{k}} | \partial_{\lambda}u_{\mathbf{k}} \rangle$ . Now first-order perturbation theory yields  $\langle \partial_{\lambda}u_{\mathbf{k}} | \partial_{\lambda}u_{\mathbf{k}} \rangle = |\langle v_{\mathbf{k}} | \partial_{\lambda}H | u_{\mathbf{k}} \rangle|^2 / (\epsilon_{1,\mathbf{k}} - \epsilon_{0,\mathbf{k}})^2$ , where  $|v_{\mathbf{k}}\rangle$  is the higher band wavefunction, and  $\epsilon_{0,\mathbf{k}}$  ( $\epsilon_{1,\mathbf{k}}$ ) is the lower (higher) band single-particle energy corresponding to crystal momentum  $\mathbf{k}$ . Now we can bound  $F_{|u_{\mathbf{k}}\rangle}$  by  $4 \langle \partial_{\lambda}u_{\mathbf{k}} | \partial_{\lambda}u_{\mathbf{k}} \rangle \leq 4 \|\partial_{\lambda}H_{\mathbf{k}}\|^2 / \Delta E^2$ , where  $\Delta E$  is the band gap, and  $\|\bullet\|$  denotes the operator norm. Furthermore,  $\|H_{\mathbf{k}}\| \leq \sup \|\partial_{\lambda}H_{\mathbf{k}}\| = \|\partial_{\lambda}H\|$ , which yields  $\langle \partial_{\lambda}u_{\mathbf{k}} | \partial_{\lambda}u_{\mathbf{k}} \rangle \leq \|\partial_{\lambda}H\|^2 / \Delta E^2$ . This proves that QFI of  $|\Psi_{\text{GS}}^{\text{PBC}}\rangle$  scales at most linearly with the system size ( $O(N) = O(V)$ ) away from TPT. This is in stark contrast with the constant scaling of QFI for the edge states.

For the specific example of the ground state of the SSH Hamiltonian, linear scaling may be explicitly proved in the continuum limit  $L \rightarrow \infty$  away from TPT (see SM [53]), and the corresponding QFI is given by

$$\lim_{L \rightarrow \infty} \frac{F_{\text{PBC}}^{\text{SSH}}(\lambda)}{L} = \begin{cases} 1/2(1 - \lambda^2) & \text{if } \lambda < 1, \\ 1/2(\lambda^4 - \lambda^2) & \text{if } \lambda > 1, \end{cases} \quad (14)$$

We further provide numerical confirmations by repeating the fitting procedure mentioned before to support our results. The scaling exponents versus  $\lambda$  are shown in Figs. 2(a)-(b) for the SSH and the Chern insulator model respectively. Expectedly, the  $\Omega(L^2)$  scaling at TPT and  $O(L^D)$  scaling far enough away are independent of the boundary conditions. For the Chern insulator, true OBC are numerically intractable beyond small system sizes, hence we use strip geometry, which leads to the small discrepancies with the PBC results.

*Conclusion.*— Through analytical investigation, we show that one can achieve precision beyond the standard limit at the transition point of free-fermionic topological models. This paves the way for development of topological quantum sensors, which are expected to be robust against local perturbations. From a fundamental point of view, our analysis indicates that gap closing, rather than long range correlation and spontaneous symmetry-breaking, is essential for obtaining quantum enhanced precision. This observation is consistent with recent discovery of quantum enhanced sensitivity at Floquet gap closing [7, 29] in periodically driven systems.

AB acknowledges support from the National Key R&D

Program of China (Grant No. 2018YFA0306703), National Science Foundation of China (Grants No. 12050410253 and No. 92065115) and the Ministry of Science and Technology of China (Grant No. QNJ2021167001L). SS acknowledges support by Alberta Major Innovation Fund. CM acknowledges Slovak Academy of Sciences for funding from HO-QIT (VEGA 2/0161/19) and OPTIQUITE (APVV-18-0518) projects, and the Stefan Schwarz Support Fund. AA acknowledges support by Killam Trusts (Postdoctoral Fellowship).

\* saubhik.sarkar@ucalgary.ca

† chiranjib.mukhopadhyay@savba.sk

‡ abhijeet.alase1@ucalgary.ca

§ abolfazl.bayat@uestc.edu.cn

- [1] C. L. Degen, F. Reinhard, and P. Cappellaro, *Rev. Mod. Phys.* **89**, 035002 (2017).
- [2] M. G. Paris, *Int. J. Quantum Inf.* **7**, 125 (2009).
- [3] M. M. Rams, P. Sierant, O. Dutta, P. Horodecki, and J. Zakrzewski, *Phys. Rev. X* **8**, 021022 (2018).
- [4] L. Gong and P. Tong, *Phys. Rev. B* **78**, 115114 (2008).
- [5] S.-J. Gu, H.-M. Kwok, W.-Q. Ning, and H.-Q. Lin, *Phys. Rev. B* **77**, 245109 (2008).
- [6] S. Greschner, A. Kolezhuk, and T. Vekua, *Phys. Rev. B* **88**, 195101 (2013).
- [7] U. Mishra and A. Bayat, *Phys. Rev. Lett.* **127**, 080504 (2021).
- [8] L. Garbe, O. Abah, S. Felicetti, and R. Puebla, [arXiv:2112.11264](https://arxiv.org/abs/2112.11264) (2021).
- [9] V. Giovannetti, S. Lloyd, and L. Maccone, *Science* **306**, 1330 (2004).
- [10] V. Giovannetti, S. Lloyd, and L. Maccone, *Phys. Rev. Lett.* **96**, 010401 (2006).
- [11] F. Fröwis and W. Dür, *Phys. Rev. Lett.* **106**, 110402 (2011).
- [12] R. Demkowicz-Dobrzański, J. Kołodyński, and M. Guţă, *Nat. Commun.* **3**, 1 (2012).
- [13] K. Wang, X. Wang, X. Zhan, Z. Bian, J. Li, B. C. Sanders, and P. Xue, *Phys. Rev. A* **97**, 042112 (2018).
- [14] H. Kwon, K. C. Tan, T. Volkoff, and H. Jeong, *Phys. Rev. Lett.* **122**, 040503 (2019).
- [15] P. Zanardi and N. Paunković, *Phys. Rev. E* **74**, 031123 (2006).
- [16] P. Zanardi, H. Quan, X. Wang, and C. Sun, *Phys. Rev. A* **75**, 032109 (2007).
- [17] P. Zanardi, M. G. Paris, and L. C. Venuti, *Phys. Rev. A* **78**, 042105 (2008).
- [18] C. Invernizzi, M. Korbman, L. C. Venuti, and M. G. Paris, *Phys. Rev. A* **78**, 042106 (2008).
- [19] S.-J. Gu, *Int. J. Mod. Phys. B* **24**, 4371 (2010).
- [20] S. Gammelmark and K. Mølmer, *New J. Phys.* **13**, 053035 (2011).
- [21] Y. Chu, S. Zhang, B. Yu, and J. Cai, *Phys. Rev. Lett.* **126**, 010502 (2021).
- [22] R. Liu, Y. Chen, M. Jiang, X. Yang, Z. Wu, Y. Li, H. Yuan, X. Peng, and J. Du, *npj Quantum Inf.* **7**, 1 (2021).
- [23] V. Montenegro, U. Mishra, and A. Bayat, *Phys. Rev. Lett.* **126**, 200501 (2021).
- [24] M. Skotiniotis, P. Sekatski, and W. Dür, *New J. Phys.* **17**, 073032 (2015).
- [25] S. Boixo, S. T. Flammia, C. M. Caves, and J. M. Geremia, *Phys. Rev. Lett.* **98**, 090401 (2007).
- [26] A. De Pasquale, D. Rossini, P. Facchi, and V. Giovannetti, *Phys. Rev. A* **88**, 052117 (2013).
- [27] S. Pang and T. A. Brun, *Phys. Rev. A* **90**, 022117 (2014).
- [28] J. Kołodyński and R. Demkowicz-Dobrzański, *New J. Phys.* **15**, 073043 (2013).
- [29] U. Mishra and A. Bayat, [arXiv:2105.13507](https://arxiv.org/abs/2105.13507) (2021).
- [30] A. Kitaev, *AIP Conference Proceedings* **1134**, 22 (2009).
- [31] S. Ryu, A. P. Schnyder, A. Furusaki, and A. W. W. Ludwig, *New J. Phys.* **12**, 065010 (2010).
- [32] B. A. Bernevig, *Topological insulators and topological superconductors* (Princeton university press, 2013).
- [33] E. Prodan and H. Schulz-Baldes, *Bulk and boundary invariants for complex topological insulators* (Springer, Switzerland, 2016).
- [34] A. Alldrige, C. Max, and M. R. Zirnbauer, *Commun. Math. Phys.* **377**, 1761 (2020).
- [35] A. Alase, *Boundary Physics and Bulk-Boundary Correspondence in Topological Phases of Matter* (Springer, Cham, 2019).
- [36] X. Chen, Z.-C. Gu, Z.-X. Liu, and X.-G. Wen, *Phys. Rev. B* **87**, 155114 (2013).
- [37] J. C. Budich and E. J. Bergholtz, *Phys. Rev. Lett.* **125**, 180403 (2020).
- [38] L. Pezze, M. Gabbriellini, L. Lepori, and A. Smerzi, *Phys. Rev. Lett.* **119**, 250401 (2017).
- [39] Y.-R. Zhang, Y. Zeng, H. Fan, J. You, and F. Nori, *Phys. Rev. Lett.* **120**, 250501 (2018).
- [40] J. Lambert and E. S. Sørensen, *Phys. Rev. B* **102**, 224401 (2020).
- [41] S. Yin, J. Song, Y. Zhang, and S. Liu, *Phys. Rev. B* **100**, 184417 (2019).
- [42] M. Chen, B. Wang, and W. Cheng, *Int. J. Theor. Phys.* , 1 (2021).
- [43] Y.-R. Zhang, Y. Zeng, T. Liu, H. Fan, J. You, and F. Nori, [arXiv:2109.03315](https://arxiv.org/abs/2109.03315) (2021).
- [44] K. v. Klitzing, G. Dorda, and M. Pepper, *Phys. Rev. Lett.* **45**, 494 (1980).
- [45] B. A. Bernevig, T. L. Hughes, and S.-C. Zhang, *Science* **314**, 1757 (2006).
- [46] N. Cooper, J. Dalibard, and I. Spielman, *Rev. Mod. Phys.* **91**, 015005 (2019).
- [47] T. Ozawa, H. M. Price, A. Amo, N. Goldman, M. Hafezi, L. Lu, M. C. Rechtsman, D. Schuster, J. Simon, O. Zilberberg, and I. Carusotto, *Rev. Mod. Phys.* **91**, 015006 (2019).
- [48] A. Alase, E. Cobanera, G. Ortiz, and L. Viola, *Phys. Rev. Lett.* **117**, 076804 (2016).
- [49] A. Alase, E. Cobanera, G. Ortiz, and L. Viola, *Phys. Rev. B* **96**, 195133 (2017).
- [50] E. Cobanera, A. Alase, G. Ortiz, and L. Viola, *J. Phys. A: Math. Theor.* **50**, 195204 (2017).
- [51] E. Cobanera, A. Alase, G. Ortiz, and L. Viola, *Phys. Rev. B* **98**, 245423 (2018).
- [52] A. Y. Kitaev, *Physics-uspekhi* **44**, 131 (2001).
- [53] (See supplemental material).
- [54] G. Brassard and P. Bratley, *Fundamentals of algorithmics* (Prentice-Hall, Inc., 1996).
- [55] N. W. Ashcroft and N. D. Mermin, *Solid State Physics* (Saunders College Publishing, 1976).
- [56] W. P. Su, J. R. Schrieffer, and A. J. Heeger, *Phys. Rev. Lett.* **42**, 1698 (1979).
- [57] M. Atala, M. Aidelsburger, J. T. Barreiro, D. Abanin, T. Kitagawa, E. Demler, and I. Bloch, *Nat. Phys.* **9**, 795 (2013).
- [58] This assumption leads to special boundary conditions as discussed in Appendix E of Ref. [51]. These boundary conditions are different from the open boundary conditions discussed in Eq. (1), but it does not change the form of edge states in Eq. (2).

- [59] M. Zaimi, C. Boudreault, N. Baspin, N. Delnour, H. Eleuch, R. MacKenzie, and M. Hilke, *Phys. Lett. A* **388**, 127035 (2021).
- [60] Z. Wu, L. Zhang, W. Sun, X.-T. Xu, B.-Z. Wang, S.-C. Ji, Y. Deng, S. Chen, X.-J. Liu, and J.-W. Pan, *Science* **354**, 83 (2016).
- [61] D. Sticlet, F. Piéchon, J.-N. Fuchs, P. Kalugin, and P. Simon, *Phys. Rev. B* **85**, 165456 (2012).
- [62] W.-W. Zhang, B. C. Sanders, S. Apers, S. K. Goyal, and D. L. Feder, *Phys. Rev. Lett.* **119**, 197401 (2017).
- [63] R. Barnett, *Phys. Rev. A* **88**, 063631 (2013).
- [64] H. Schomerus, *Opt. Lett.* **38**, 1912 (2013).
- [65] C. Poli, M. Bellec, U. Kuhl, F. Mortessagne, and H. Schomerus, *Nature Communications* **6**, 6710 (2015).
- [66] B. Galilo, D. K. K. Lee, and R. Barnett, *Phys. Rev. Lett.* **115**, 245302 (2015).
- [67] A. L. Fetter and J. D. Walecka, *Quantum theory of many-particle systems* (Courier Corporation, 2012).

## SUPPLEMENTAL MATERIAL

### QFI of edge states with unconstrained $z$

In this section, we derive the scaling of QFI for general edge states with complex values of  $z$ . For  $z = re^{i\theta}$ , we can express  $|\partial_\lambda \phi_z\rangle = (\partial_\lambda r) |\partial_r \phi_z\rangle + (\partial_\lambda \theta) |\partial_\theta \phi_z\rangle$ . Then the QFI of  $|\phi_z\rangle$  can be expressed as

$$F_{|\phi_z\rangle}(\lambda) = \begin{bmatrix} (\partial_\lambda r) & (\partial_\lambda \theta) \end{bmatrix} \begin{bmatrix} F_{|\phi_z\rangle}(r, r) & F_{|\phi_z\rangle}(r, \theta) \\ F_{|\phi_z\rangle}(\theta, r) & F_{|\phi_z\rangle}(\theta, \theta) \end{bmatrix} \begin{bmatrix} (\partial_\lambda r) \\ (\partial_\lambda \theta) \end{bmatrix}, \quad (\text{S1})$$

where

$$\begin{aligned} F_{|\phi_z\rangle}(r, r) &= 4 \left( \langle \partial_r \phi_z | \partial_r \phi_z \rangle - \langle \partial_r \phi_z | \phi_z \rangle \langle \phi_z | \partial_r \phi_z \rangle \right), \\ F_{|\phi_z\rangle}(r, \theta) &= 4 \left( \langle \partial_r \phi_z | \partial_\theta \phi_z \rangle - \langle \partial_r \phi_z | \phi_z \rangle \langle \phi_z | \partial_\theta \phi_z \rangle \right), \\ F_{|\phi_z\rangle}(\theta, r) &= 4 \left( \langle \partial_\theta \phi_z | \partial_r \phi_z \rangle - \langle \partial_\theta \phi_z | \phi_z \rangle \langle \phi_z | \partial_r \phi_z \rangle \right), \\ F_{|\phi_z\rangle}(\theta, \theta) &= 4 \left( \langle \partial_\theta \phi_z | \partial_\theta \phi_z \rangle - \langle \partial_\theta \phi_z | \phi_z \rangle \langle \phi_z | \partial_\theta \phi_z \rangle \right). \end{aligned} \quad (\text{S2})$$

We now use an elegant trick to calculate all quantities on the right-hand side of Eq. (S2). First define  $|\tilde{\phi}_z\rangle = \sum_{j \in [L]} z^j |j\rangle$  so that  $|\phi_z\rangle = |\tilde{\phi}_z\rangle / \|\tilde{\phi}_z\rangle\|$ . Some straightforward algebra reveals

$$F_{|\phi_z\rangle}(r, r) = 4 \frac{\langle \partial_r \tilde{\phi}_z | \partial_r \tilde{\phi}_z \rangle}{\|\tilde{\phi}_z\rangle\|^2} - 4 \frac{\langle \partial_r \tilde{\phi}_z | \tilde{\phi}_z \rangle \langle \tilde{\phi}_z | \partial_r \tilde{\phi}_z \rangle}{\|\tilde{\phi}_z\rangle\|^4}, \quad (\text{S3})$$

and similar identities hold for  $F_{|\phi_z\rangle}(r, \theta)$ ,  $F_{|\phi_z\rangle}(\theta, r)$ , and  $F_{|\phi_z\rangle}(\theta, \theta)$ . Now observe that

$$|\partial_r \tilde{\phi}_z\rangle = \sum_{j \in [L]} jr^{j-1} e^{i\theta j} |j\rangle = \frac{-i}{r} \sum_{j \in [L]} ijr^j e^{i\theta j} |j\rangle = \frac{-i}{r} |\partial_\theta \tilde{\phi}_z\rangle. \quad (\text{S4})$$

Therefore, we get

$$\begin{aligned} F_{|\phi_z\rangle}(\lambda) &= F_{|\phi_z\rangle}(r, r) \begin{bmatrix} (\partial_\lambda r) & (\partial_\lambda \theta) \end{bmatrix} \begin{bmatrix} 1 & -i/r \\ i/r & 1/r^2 \end{bmatrix} \begin{bmatrix} (\partial_\lambda r) \\ (\partial_\lambda \theta) \end{bmatrix} \\ &= F_{|\phi_z\rangle}(r, r) [(\partial_\lambda r)^2 + (\partial_\lambda \theta)^2]. \end{aligned} \quad (\text{S5})$$

Note that  $F_{|\phi_z\rangle}(r, r) = F_{|\phi_z\rangle}(r)$ , and the latter was calculated in the main text to yield

$$F_{|\phi_z\rangle}(r) = \frac{4[1 + r^{4L} - r^{2L-2}(2r^2 + L^2(1 - r^2)^2)]}{(1 - r^2)^2(1 - r^{2L})^2}. \quad (\text{S6})$$

Away from TPT ( $\lambda \neq \lambda_c$ ), we have  $r < 1$  and therefore  $F_{|\phi_z\rangle}(r) \in \Theta(1)$  so that  $F_{|\phi_z\rangle}(\lambda) \in \Theta(1)$  as well. As TPT is approached, ( $\lambda \rightarrow \lambda_c$ ), we have  $r \rightarrow 1$ . In this limit,

$$\lim_{r \rightarrow 1} F_{|\phi_z\rangle}(r) = \frac{L^2 - 1}{3}. \quad (\text{S7})$$

Finally substituting this value in Eq. (S5), we obtain

$$\lim_{\lambda \rightarrow \lambda_c} F_{|\phi_z\rangle}(\lambda) = \frac{(L^2 - 1)[(\partial_\lambda r)^2 + (\partial_\lambda \theta)^2]}{3} \implies F_{|\phi_z\rangle}(\lambda_c) \in \Theta(L^2). \quad (\text{S8})$$

### Optimal measurement for the general edge state

In this section, we show that the projective measurement described by projectors  $\{|j\rangle\langle j| \otimes \mathbb{1}, j \in [L]\}$  is optimal up to a length-independent prefactor if  $\arg(z)$  also depends on  $\lambda$ .

We first prove that, if a quantum state  $|\psi(\lambda)\rangle$  is expressed in a basis  $|e_j\rangle$  has all real coefficients, then QFI  $F_{|\psi\rangle}^Q(\lambda) = F_{|\psi\rangle}^C(\lambda)$ , with  $F_{|\psi\rangle}^C(\lambda)$  denoting the CFI with of the probability distribution  $\{p_j = |\langle\psi|e_j\rangle|^2\}$ . To prove this statement, we express  $|\psi\rangle = \sum_j \sqrt{p_j} |e_j\rangle$ , so that  $|\partial_\lambda\psi\rangle = \sum_j (\partial_\lambda p_j / 2\sqrt{p_j}) |e_j\rangle$ . Note that  $\langle\psi|\partial_\lambda\psi\rangle = 0$ , so that  $F_{|\psi\rangle}^Q(\lambda) = 4 \langle\partial_\lambda\psi|\partial_\lambda\psi\rangle$ . Now

$$F_{|\psi\rangle}^Q(\lambda) = 4 \langle\partial_\lambda\psi|\partial_\lambda\psi\rangle = 4 \sum_j \frac{(\partial_\lambda p_j)^2}{4p_j} = \sum_j p_j \left( \frac{\partial_\lambda p_j}{p_j} \right)^2 = \sum_j p_j (\partial_\lambda \ln p_j)^2 = F_{|\psi\rangle}^C(\lambda). \quad (\text{S9})$$

Next, observe that this result holds also under a milder assumption on  $|\psi\rangle$ , namely that  $\langle\psi|e_j\rangle$  is complex but  $\arg(\langle\psi|e_j\rangle)$  is independent of  $\lambda$ . Using this result for  $|\psi\rangle = |\phi_z\rangle$  and  $\{|e_j\rangle = |j\rangle\}$ , we get QFI  $F_{|\phi_z\rangle}(r) = F_{|\phi_z\rangle}^C(r)$ . Then by Eq. (S5), we get for the general case, where  $\arg(z)$  also depends on  $\lambda$ ,

$$F_{|\phi_z\rangle}(\lambda) = F_{|\phi_z\rangle}^C(\lambda) \left( 1 + \frac{(\partial_\lambda \theta)^2}{r^2 (\partial_\lambda r)^2} \right). \quad (\text{S10})$$

Finally we have QFI for the edge state  $F_{|\psi_{\text{edge}}\rangle}(\lambda) = F_{|\phi_z\rangle}(\lambda) + F_{|u\rangle}(\lambda)$  and  $F_{|\psi_{\text{edge}}\rangle}^C(\lambda) = F_{|\phi_z\rangle}^C(\lambda)$ , which leads to

$$F_{|\psi_{\text{edge}}\rangle}(\lambda) = F_{|\psi_{\text{edge}}\rangle}^C(\lambda) \left( 1 + \frac{(\partial_\lambda \theta)^2}{r^2 (\partial_\lambda r)^2} \right) + F_{|u\rangle}(\lambda). \quad (\text{S11})$$

Observe that  $\left( 1 + \frac{(\partial_\lambda \theta)^2}{r^2 (\partial_\lambda r)^2} \right)$  and  $F_{|u\rangle}(\lambda)$  do not depend on  $L$ . Hence, for every value of the parameter  $\lambda$ , the position measurement is optimal up to a constant prefactor and an additive constant independent of  $L$ .

### QFI of many-body Slater determinant states

Starting with the expression for the Slater determinant state  $|\Psi\rangle$  in the main text we now calculate the QFI using the standard formula

$$F_{|\Psi\rangle} = 4 \left( \langle\partial_\lambda\Psi|\partial_\lambda\Psi\rangle - |\langle\partial_\lambda\Psi|\Psi\rangle|^2 \right). \quad (\text{S12})$$

To calculate the first term, we proceed as

$$\langle\partial_\lambda\Psi|\partial_\lambda\Psi\rangle = \frac{1}{N!} \sum_{\sigma, \tau \in S_N} \text{sgn}(\sigma\tau) \sum_{l, l'=1}^N \left( \langle\psi_{\tau_1}|\dots\langle\partial_\lambda\psi_{\tau_l}|\dots\langle\psi_{\tau_N}|\right) \left( |\psi_{\sigma_1}\rangle\dots\langle\partial_\lambda\psi_{\sigma_{l'}}|\dots\langle\psi_{\sigma_N}|\right). \quad (\text{S13})$$

Note that if  $l = l'$ , then the non-zero terms correspond to  $\sigma = \tau$ . On the other hand, if  $l \neq l'$ , then non-zero terms correspond to  $\sigma = \tau$  and  $\sigma = \tau(l'l')$ , where  $(l'l')$  is the permutation that exchanges the indices  $l$  and  $l'$ . In the latter case, we have  $\text{sgn}(\sigma\tau) = -1$ . These observations lead to

$$\begin{aligned} \langle\partial_\lambda\Psi|\partial_\lambda\Psi\rangle &= \frac{1}{N!} \sum_{\sigma \in S_N} \left( \sum_{l=1}^N \langle\partial_\lambda\psi_{\sigma_l}|\partial_\lambda\psi_{\sigma_l}\rangle + \sum_{l \neq l'} \langle\partial_\lambda\psi_{\sigma_l}|\psi_{\sigma_l}\rangle \langle\psi_{\sigma_{l'}}|\partial_\lambda\psi_{\sigma_{l'}}\rangle - \sum_{l \neq l'} \langle\partial_\lambda\psi_{\sigma_l}|\psi_{\sigma_{l'}}\rangle \langle\psi_{\sigma_{l'}}|\partial_\lambda\psi_{\sigma_l}\rangle \right) \\ &= \sum_{l=1}^N \langle\partial_\lambda\psi_l|\partial_\lambda\psi_l\rangle - \sum_{l \neq l'} \langle\partial_\lambda\psi_l|\psi_l\rangle \langle\partial_\lambda\psi_{l'}|\psi_{l'}\rangle - \sum_{l \neq l'} \langle\partial_\lambda\psi_l|\psi_{l'}\rangle \langle\psi_{l'}|\partial_\lambda\psi_l\rangle. \end{aligned} \quad (\text{S14})$$

We similarly calculate the second term on the right-hand side of Eq. (S12), which yields

$$\langle\partial_\lambda\Psi|\Psi\rangle^2 = \left( \sum_{l=1}^N \langle\partial_\lambda\psi_l|\psi_l\rangle \right)^2 = \sum_{l \neq l'} \langle\partial_\lambda\psi_l|\psi_l\rangle \langle\partial_\lambda\psi_{l'}|\psi_{l'}\rangle + \sum_l \langle\partial_\lambda\psi_l|\psi_l\rangle^2. \quad (\text{S15})$$

Substituting Eqs. (S14) and (S15) in Eq. (S12) yields

$$\begin{aligned} F_{|\Psi\rangle} &= 4 \left( \sum_{l=1}^N \langle\partial_\lambda\psi_l|\partial_\lambda\psi_l\rangle - \sum_{l \neq l'} \langle\partial_\lambda\psi_l|\psi_{l'}\rangle \langle\psi_{l'}|\partial_\lambda\psi_l\rangle + \sum_l \langle\partial_\lambda\psi_l|\psi_l\rangle^2 \right) \\ &= 4 \sum_l \langle\partial_\lambda\psi_l|\mathbb{1} - P|\partial_\lambda\psi_l\rangle, \end{aligned} \quad (\text{S16})$$



where  $P$  is the projector on the occupied states, i.e.  $P = \sum_{l=1}^N |\psi_l\rangle \langle \psi_l|$ . Now observe that  $(\mathbb{1} - P)|\psi_l\rangle = 0$  for all  $l$ , hence we can further express

$$\begin{aligned} F_{|\Psi\rangle} &= 4\text{Tr} \left[ (\mathbb{1} - P) \left( \sum_l |\partial_\lambda \psi_l\rangle \langle \partial_\lambda \psi_l| \right) \right] \\ &= 2\text{Tr} \left[ (\mathbb{1} - P) \partial^2 P \right]. \end{aligned} \quad (\text{S17})$$

### Many-body QFI scaling at TPT for SSH Hamiltonian (PBC)

The SSH Hamiltonian in Eq. (6) in the main text can be rewritten in the momentum space with the following form of the Bloch Hamiltonian corresponding to momentum  $k = 2\pi\kappa/L$

$$H_k^{\text{SSH}} = - \begin{bmatrix} 0 & J_1 + J_2 e^{-i2\pi\kappa/L} \\ J_1 + J_2 e^{i2\pi\kappa/L} & 0 \end{bmatrix}. \quad (\text{S18})$$

For the filled lower band, we have

$$|u_k\rangle = \frac{1}{\sqrt{2}} \begin{bmatrix} 1 \\ e^{i\phi_k} \end{bmatrix}, \quad e^{2i\phi_k} = \frac{\lambda + e^{i2\pi\kappa/L}}{\lambda + e^{-i2\pi\kappa/L}}, \quad (\text{S19})$$

and

$$|\partial_\lambda u_k\rangle = \frac{\partial_\lambda \phi_k}{\sqrt{2}} \begin{bmatrix} 0 \\ i e^{i\phi_k} \end{bmatrix}. \quad (\text{S20})$$

We obtain

$$F_{|u_k\rangle} = 2(\partial_\lambda \phi_k)^2 + 4(i\partial_\lambda \phi_k/2)^2 = (\partial_\lambda \phi_k)^2. \quad (\text{S21})$$

At the Dirac point, which is  $\kappa = L/2$ , we obtain  $\phi_k = 0$  independent of  $\lambda$ , and therefore  $F_{|u_{N/2}\rangle} = 0$ . To proceed further, we can differentiate the expression for  $e^{2i\phi_k}$  for  $\kappa \neq L/2$ , which yields

$$2ie^{2i\phi_k} \partial_\lambda \phi_k = \frac{1}{\lambda + e^{-i2\pi\kappa/L}} - \frac{\lambda + e^{i2\pi\kappa/L}}{(\lambda + e^{-i2\pi\kappa/L})^2} = -\frac{2i \sin(2\pi\kappa/L)}{(1 + \lambda e^{-i2\pi\kappa/L})^2}. \quad (\text{S22})$$

Therefore,

$$\partial_\lambda \phi_k = -\frac{\sin(2\pi\kappa/L)}{1 + \lambda^2 + 2\lambda \cos(2\pi\kappa/L)}. \quad (\text{S23})$$

At  $\lambda = 1$ , we can further simplify this expression to

$$\partial_\lambda \phi_k = -\frac{\sin(2\pi\kappa/L)}{2(1 + \cos(2\pi\kappa/L))} = -\frac{\tan(\pi\kappa/L)}{2}, \quad (\text{S24})$$

and therefore  $F_{|u_k\rangle} = \tan^2(\pi\kappa/L)/4$ . Finally, the QFI of the many-body ground state is obtained by summing over QFI of all  $|u_k\rangle$  except at the Dirac point, which is  $\kappa = L/2$ . We therefore get

$$F_{\text{PBC}}^{\text{SSH}}(\lambda_c) = \sum_{\kappa=1}^{L-1} \frac{\cot^2(\pi\kappa/L)}{4} = \frac{L^2 - 3L + 2}{12}, \quad (\text{S25})$$

where the last equation is obtained using Mathematica. We therefore have proven  $\Theta(N^2)$  dependence for the QFI of  $|\Psi_{\text{GS}}^{\text{PBC}}\rangle$  for the SSH Hamiltonian.

### Many-body QFI scaling away from TPT for SSH (PBC)

We have already shown that QFI scales at most linearly away from TPT for the SSH ground state. In the *continuum* limit, i.e.,  $L \rightarrow \infty$ , we may prove this rigorously in the following way. QFI  $F_{\text{PBC}}^{\text{SSH}}(\lambda)$  is given by  $(\partial_\lambda \phi_\kappa)^2$  summed over all modes  $\kappa \in [1, L]$ , i.e.,

$$F_{\text{PBC}}^{\text{SSH}}(\lambda) = \sum_{\kappa=1}^L \left( \frac{\sin(2\pi\kappa/L)}{1 + \lambda^2 + 2\lambda \cos(2\pi\kappa/L)} \right)^2. \quad (\text{S26})$$

In the continuum limit, this sum may be approximated by an integral if the function is Riemann-Integrable. That is,

$$F_{\text{PBC}}^{\text{SSH}}(\lambda) = \frac{L}{\pi} \int_0^{\frac{\pi}{2}-\epsilon} \left( \frac{\sin x}{1 + \lambda^2 + 2\lambda \cos x} \right)^2 dx + \frac{L}{2\pi} \int_{\frac{\pi}{2}+\epsilon}^{2\pi} \left( \frac{2 \sin x}{1 + \lambda^2 + 2\lambda \cos x} \right)^2 dx. \quad (\text{S27})$$

Note that we have divided the domain of integration into two discontinuous domains to reflect the physics at the Dirac Point. It is easy to see that if this integral exists, then QFI scales linearly with  $L$ . This is the case away from TPT, where QFI takes the following form

$$\lim_{L \rightarrow \infty} \frac{F_{\text{PBC}}^{\text{SSH}}(\lambda)}{L} = \begin{cases} \frac{1}{2(1-\lambda^2)} & \text{if } \lambda < 1, \\ \frac{1}{2(\lambda^4-\lambda^2)} & \text{if } \lambda > 1, \end{cases} \quad (\text{S28})$$

At TPT, the functions are no longer piecewise Riemann Integrable and linear scaling no longer applies. This is consistent with the quadratic scaling derived above.

### Many-body QFI scaling at TPT for Chern insulator (PBC)

For the Chern insulator Hamiltonian in Eq. (7) in the main text, the lower-band eigenvectors are given by,

$$|\psi_{\mathbf{k}}\rangle = |\mathbf{k}\rangle |u_{\mathbf{k}}\rangle, \quad (\text{S29})$$

with

$$|u_{\mathbf{k}}\rangle = \sqrt{\frac{B_z + E_{\mathbf{k}}}{2E_{\mathbf{k}}}} \begin{bmatrix} \frac{B_z - E_{\mathbf{k}}}{B_x + iB_y} \\ 1 \end{bmatrix}, \quad (\text{S30})$$

where  $E_{\mathbf{k}} = \sqrt{B_x^2 + B_y^2 + B_z^2}$  is the magnitude of eigenenergy. After a bit of algebra one finds

$$|\partial_\lambda u_{\mathbf{k}}\rangle = \sqrt{\frac{B_z + E_{\mathbf{k}}}{2E_{\mathbf{k}}}} \frac{E_{\mathbf{k}} - B_z}{2E_{\mathbf{k}}^2} \begin{bmatrix} \frac{B_z - E_{\mathbf{k}}}{B_x + iB_y} \\ 1 \end{bmatrix}, \quad (\text{S31})$$

which is orthogonal to  $|u_{\mathbf{k}}\rangle$ . Therefore we get

$$F_{\text{PBC}}^{\text{Ch}}(\lambda) = \sum_{\mathbf{k}} \langle \partial_\lambda u_{\mathbf{k}} | \partial_\lambda u_{\mathbf{k}} \rangle = \sum_{\mathbf{k}} \frac{B_x^2 + B_y^2}{4E_{\mathbf{k}}^4}. \quad (\text{S32})$$

We use this expression in the main text to extract the scaling of QFI at TPT and away from it.